NEW METHODS FOR THE ANALYSIS OF ESR POWDER PATTERNS

Janice A. DeGray and Philip H. Rieger

Department of Chemistry
Brown University
Providence, Rhode Island 02912

INTRODUCTION

Electron spin resonance spectroscopy is an important tool in the study of organometallic reactions initiated by electron transfer. For example, when an acetylene-bridged dicobalt hexacarbonyl, $(R_2C_2)Co_2(CO)_6$, is reduced by one electron in a polar aprotic solvent, the initial product is the radical anion (1). Interpretation of the powder pattern ESR spectrum of this species showed that the principal axes of the g-matrix and the two ^{59}Co hyperfine matrices were noncoincident, consistent with the presence of a bent Co–Co bond. When $(R_2C_2)Co_2(CO)_6$, R = Ph or t-Bu, is reduced at temperatures above -40°C, another radical is rapidly formed, the ESR spectrum of which shows coupling to only one ^{59}Co nucleus. Electrochemical evidence and ESR spectra of a series of related radicals convinced us that the observed species were $(R_2C_2)Co(CO)_{3-n}L_n$, (n = 0,1,2,3) where L is a phosphine, phosphite, or arsine (2). Although it is reasonable to postulate a square-planar structure for these radicals, conclusive proof of the structure came from the analysis (3) of the powder spectrum of $(Ph_2C_2)Co(CO)[P(OEt)_3]_2$, which shows the presence of *cis* and *trans* isomers, the former with two non-equivalent ^{31}P couplings, the latter with two equivalent couplings. This spectrum, shown in Figure 1, is expected to contain more than 150 features resulting from two radical species, each with a g-matrix, a ^{59}Co coupling matrix, and two ^{31}P coupling matrices.

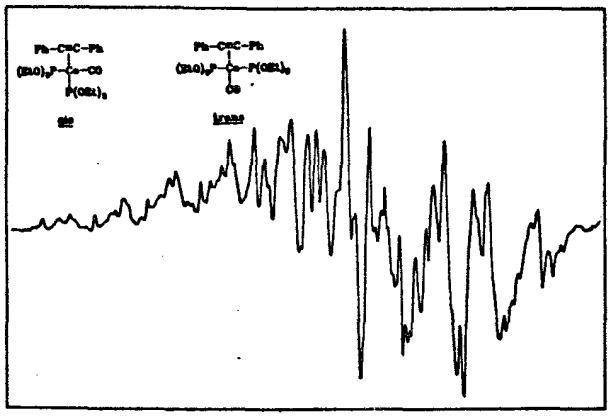

Figure 1. X-band ESR spectrum of $(Ph_2C_2)Co(CO)[P(OEt)_3]_2$ in THF at 120 K.

The traditional method of powder pattern analysis involves comparison of the experimental spectrum with a computer-simulated spectrum. The most straightforward computer simulation method (4) involves computation of the resonant magnetic field $B = B(\cos\theta, \phi, \{m_i\})$ for *ca.* 10^5 values of $\cos\theta$, ϕ for each set of nuclear spin quantum numbers. Construction of a histogram, *i.e.*, a plot of the number of times the resonant field B falls between B_i and B_{i+1} *vs.* B, gives an approximation to the unbroadened absorption spectrum (equivalent to a "stick" representation of an isotropic spectrum). The absorption spectrum is then broadened by numerical convolution with a line shape function and differentiated to give the desired simulation. Although a "cut and try" approach to spectrum analysis works reasonably well when there are small numbers of parameters, the spectrum of Figure 1 requires at least 21 parameters for simulation and analysis by this method is exceedingly tedious and very expensive in computer time. Furthermore, this approach gives no systematic way of refining parameters or of estimating the uncertainties in fitted parameters.

Faced with the need to interpret such complex powder pattern spectra, we have developed a least-squares approach to the problem which focuses on the field positions of resolved spectral features. We have found this approach very useful in the analysis of organometallic radical ESR spectra and it should be adaptable to other forms of spectroscopy where powder pattern spectra are obtained. A preliminary description of our approach was published in 1982 (5).

THE NATURE OF A POWDER PATTERN

Spectral features in a first-derivative ESR powder pattern are of three types: positive-going

features which resemble absorption lines, negative-going features which resemble emission lines, and baseline-crossing features which resemble isotropic derivative lines. Consider the simplest type of ESR powder pattern spectrum, interpretable by use of a spin Hamiltonian with only the electron Zeeman term. The resonant field then is given by

$$B = h\nu/g\mu_B$$

where ν is the microwave frequency and

$$g = (g_z^2\cos^2\theta + g_\perp^2\sin^2\theta)^{\frac{1}{2}}$$

$$g_\perp = (g_x^2\cos^2\phi + g_y^2\sin^2\phi)^{\frac{1}{2}}$$

The angles θ and ϕ describe the orientation of B in the g-matrix principal axis system. Features in the first derivative spectrum correspond to discontinuities in the absorption spectrum which arise when

$$\frac{\partial B}{\partial \theta} = \frac{h\nu}{\mu_B}\,\frac{g_z^2 - g_\perp^2}{g^3}\,\sin\theta\,\cos\theta = 0$$

and

$$\frac{\partial B}{\partial \phi} = \frac{h\nu}{\mu_B}\,\frac{g_x^2 - g_y^2}{g^3}\,\sin^2\theta\,\sin\phi\,\cos\phi = 0$$

These equations have three solutions:

$$\theta = 0$$
$$\theta = \pi/2,\ \phi = 0$$
$$\theta = \pi/2,\ \theta = \pi/2.$$

In other words, we expect to find spectral features corresponding to orientation of the magnetic field along the principal axes of the g-matrix. Indeed, three features are found in a spectrum simulation for this case, as shown in Figure 2. An equivalent way of viewing this result is to consider the surface produced when B is plotted as a function of cos θ and ϕ as shown in Figure 3. The coordinates (cos θ, ϕ) = (1,0), (0,0), and (0,π/2) are seen to correspond to the minimum resonant field, the maximum resonant field, and to a saddle point on the surface and these correspond in the spectrum of Figure 2 to the negative-going, positive-going, and baseline-crossing features, respectively.

The situation becomes somewhat more complicated when hyperfine coupling is included. With coupling to one magnetic nucleus, the

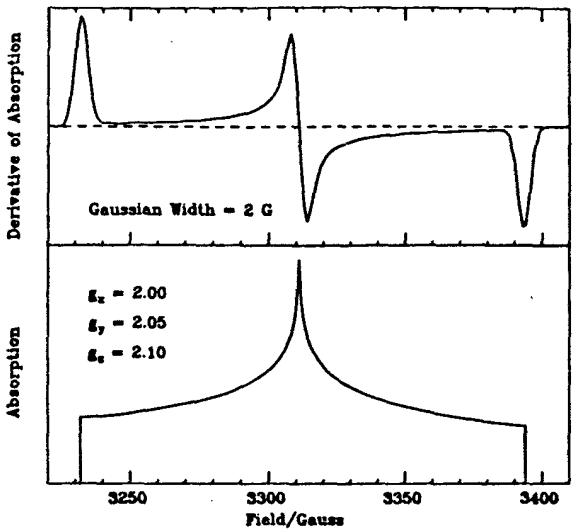

Figure 2. Simulated absorption and first-derivative spectra for a spectrum with no hyperfine coupling.

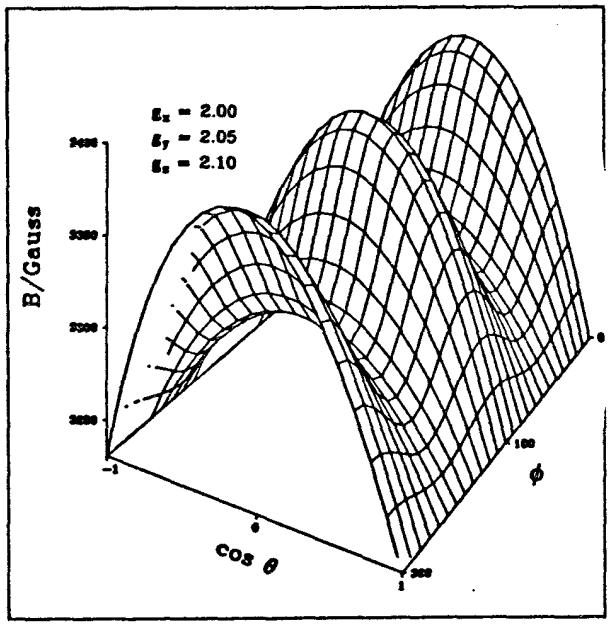

Figure 3. Plot of B *vs.* cos θ and ϕ for a spectrum with no hyperfine coupling.

resonant field is given (to first order, assuming coincident g- and hyperfine principal axes) by

$$B = h\nu/g\mu_B - Km_I/g\mu_B$$

where

$$gK = (g_z^2A_z^2\cos^2\theta + g_\perp^2A_\perp^2\sin^2\theta)^{\frac{1}{2}}$$

$$g_\perp A_\perp = (g_x^2A_x^2\cos^2\phi + g_y^2A_y^2\sin^2\phi)^{\frac{1}{2}}$$

We again expect features when B is oriented

along one of the principal axes. However, the equations, $\partial B/\partial\theta = 0$ and $\partial B/\partial\phi = 0$, may sometimes have additional solutions. Ovchinnikov and Konstantinov (6) have shown that an extra feature is expected corresponding to an orientation of B in the ij-plane when the following inequalities are satisfied:

$$2A_i^2 - \frac{h\nu A_i}{m_I} < \frac{g_i^2 A_i^2 - g_j^2 A_j^2}{g_i^2 - g_j^2} < 2A_j^2 - \frac{h\nu A_j}{m_I}$$

Thus as many as six[1] spectral features might occur for a given set of nuclear spin quantum numbers. Consider, for example, a hypothetical case with g = (1.90, 2.05, 2.12), I = 1, and A = (0, 100, 200) x 10^{-4} cm^{-1}, for which the above criterion predicts three extra features for m_I = -1. A topographic map of the B *vs.* cos θ, ϕ surface is shown in Figure 4. The global

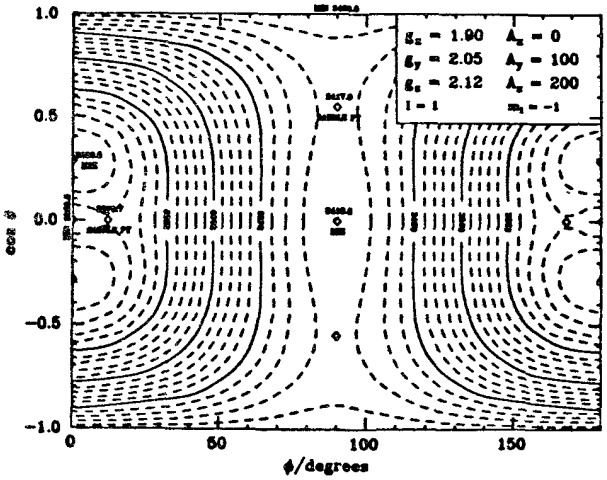

Figure 4. Topographic map showing B as a function of cos θ and ϕ for hypothetical g- and hyperfine matrices.

minimum is found for B oriented along the z-axis, but local minima also occur for B along the x- and y-axes. The global maximum corresponds to an orientation of B in the xz-plane and two saddle points are found for orientations in the yz- and xy-planes. The computer simulation of this example, shown in Figure 5, clearly shows two of the minima (positive-going features), the maximum (negative-going feature) and the two

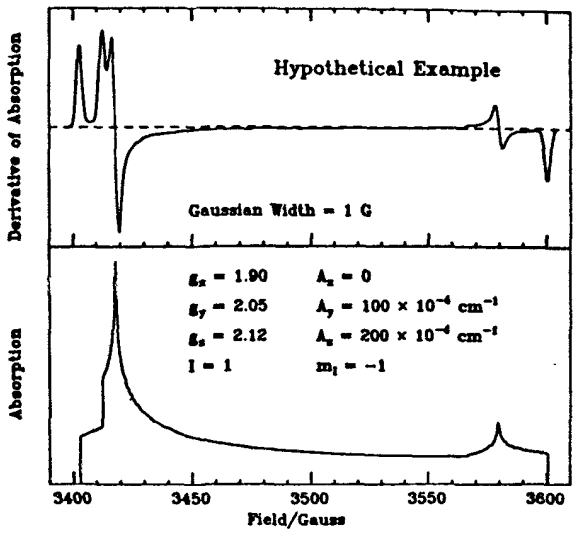

Figure 5. Simulated absorption and first-derivative spectra for the surface shown in Figure 4.

saddle points (baseline-crossing features) The mimimum corresponding to B along the x-axis is only just detectable in the simulation and probably would be missed altogether in an experimental spectrum. The topographic map of Figure 4 shows that the missing feature corresponds to a rather shallow minimum with a small number of adjacent orientations and thus to a low intensity in the spectrum.

While the analytical approach of Ovchinnikov and Konstantinov works well in simple cases, when there are two or more hyperfine couplings, when the spectrum cannot be interpreted satisfactorily using first-order perturbation theory, or when the principal axes of the g- and hyperfine matrices are non-coincident, the analytical equations become impossibly complex and a numerical method is required.

Consider, for example, a relatively simple case of non-coincident principal axes (7). The isotropic ESR spectrum of $CpCr(CO)_2NO^-$ is very similar to those of nitroxide radicals, consisting of a simple 1:1:1 triplet corresponding to coupling the unpaired electron to the ^{14}N nucleus, but the g-value, <g> = 1.990, suggests significant chromium character in the semi-occupied molecular orbital. The frozen solution spectrum, a simulation of which is shown in Figure 6, can be interpreted approximately in terms of axial g- and hyperfine coupling matrices, but with the major (parallel) axes of the g- and hyperfine matrices approximately perpendicular

[1] When second-order effects are taken into consideration, it is found that two or more extra features can occur for orientations in a single plane. In general, most of these correspond to such a small number of orientations that the effect on the absorption and first-derivative spectra is undetectable.

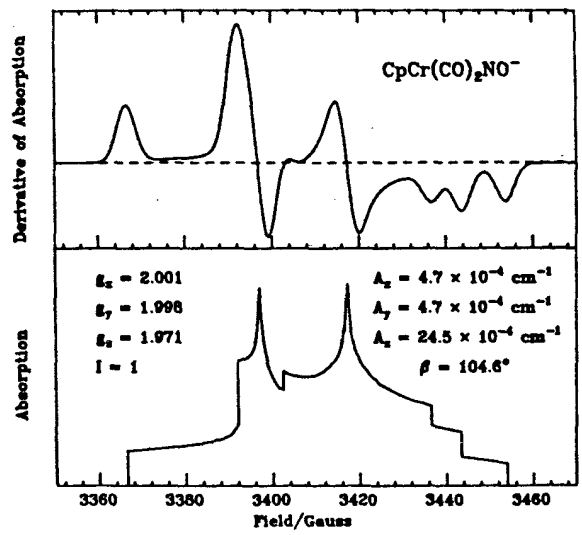

Figure 6. Simulated absorption and first-derivative spectra of $CpCr(CO)_2NO^{\cdot}$.

to one another. Furthermore, the three high-field features (which correspond to $g_{\parallel}$,$A_{\perp}$) are markedly unevenly spaced. This apparent anomaly can be explained and the spectrum satisfactorily simulated if the angle between the major axes is $\beta = 104.6°$. A topographic map of B *vs.* (cos θ, ϕ) for $m_I = -1$ is shown in Figure

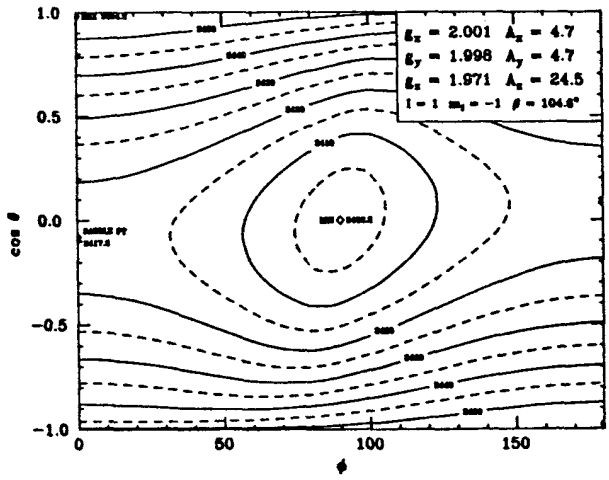

Figure 7. Topographic map of B *vs. cos* θ and ϕ for the $m_I = -1$ component of the spectrum of $CpCr(CO)_2(NO)^{\cdot}$.

7. The minimum resonant field corresponds to orientation of B along the y-axis, but the maximum and saddle point are found for orientations of B in the xz-plane near, but not coincident with, the z- and x-axes. Again these correspond to features in the spectrum. Plots for the $m_I = 0$ and $+1$ components show spectral features at similar (but slightly different) displacements of B from orientation along the z- and x-axes, thus accounting for the unequal spacings of the features in the spectrum.

COMPUTER SEARCH ALGORITHM

The above three examples illustrate the problem to be dealt with in the analysis of a powder pattern spectrum and suggest a solution. In general, three or more spectral features are expected for each set of nuclear spin quantum numbers. These features correspond to minima, maxima, or saddle points on a B *vs.* (cos θ, ϕ) surface. If B can be computed as an analytical function of these angles and the components of the g- and hyperfine matrices, a computer search of the surface for extrema should be straightforward. If we confine our interest to cases where at least one of the principal axes of the g- and hyperfine matrices is common, we can restrict the search to the xz-, yz-, and xy-planes.

The search algorithm is shown schematically is Figure 8. The resonant field is first computed

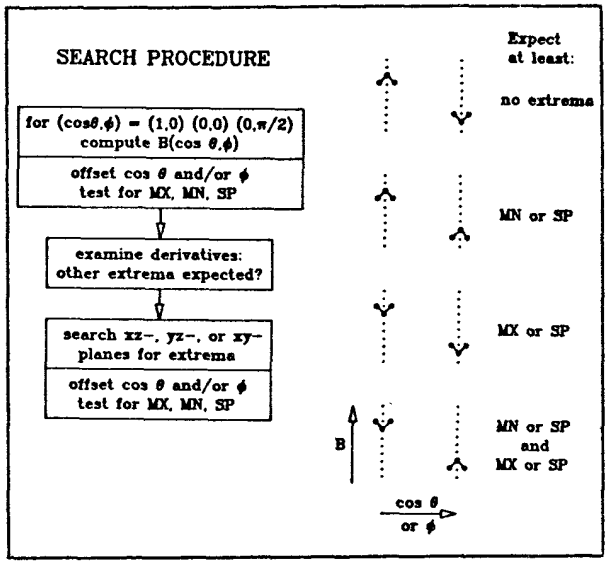

Figure 8. Schematic representation of algorithm for location of minima, maxima, and saddle points on a B *vs.* cos θ, ϕ surface.

for orientation along one of the axes (*e.g.*, the z-axis) and then for four displacements (*e.g.*, in the the positive and negative xz- and yz-planes) and the approximate derivatives, $\partial B/\partial(\cos\theta)$ or $\partial B/\partial\phi$, computed. The derivatives are then checked to determine whether B is a minimum (B increases for all displacements), a maximum (B decreases for all displacements), or a saddle point (B increases for two displacements and decreases for displacements in the perpendicular direction). This procedure is repeated for the other two axes. The derivatives obtained for the various axes are

then compared to see whether other features are expected along the xz-, yz-, or xy-planes. For example, if B increases for a displacement from $(\cos\theta,\phi) = (1,0)$ to $(1-\delta,0)$ and also increases for a displacement from (0,0) to $(\delta,0)$, then B must go through a maximum (or saddle point) somewhere in the xz-plane and a search is initiated. Starting at $\cos\theta = 1$, $\cos\theta$ is stepped by -0.1 until the extremum has been passed, the search direction is then reversed with an increment of +0.02 until the extremum is passed, and finally the search direction is reversed with an increment of -0.004. The value of $\cos\theta$ is thus determined to approximately ± 0.002. Two steps in the orthogonal direction are then used to determine whether the extremum is a maximum or a saddle point. Other outcomes of the derivative comparison step are summarized in Figure 8.

LEAST-SQUARES METHOD

In general the resonant magnetic field corresponding to the jth feature observed in an ESR powder pattern depends on the various spin Hamiltonian parameters—the components of the g- and hyperfine matrices and the Euler angles connecting the principal axes of these matrices. The feature can be assigned to a set of nuclear spin quantum numbers, $\{m_I\}$, and to a feature type—maximum, minimum, or saddle point—and, given a trial set of parameters, the field for the feature can be computed and compared with the field measured from the experimental spectrum,

$$\delta B_j = B_{expt,j} - B_{calc,j}$$

The goal of a least-squares procedure is to adjust the parameters such that the sum-of-squares

$$S = \sum_j (\delta B_j)^2$$

is minimized. The resonant field of a particular feature can also be written as a Taylor series expansion about the value calculated using the trial set of parameters:

$$B = B_{calc} + \sum_i \left(\frac{\partial B}{\partial P_i}\right) \delta P_i$$

Thus given estimates of the partial derivatives, a linear least-squares fit of δB_j to $(\partial B/\partial P_i)$ yields corrections to the parameters, δP_i. Iteration with the corrected set of parameters should then converge to the best set of parameters for the spectrum at hand. The least-squares method also can provide appropriate statistics (8) such as a variance-covariance matrix so that the significance of the fitted parameters can be properly judged.

The block diagram of a least-squares program which incorporates the above features is shown in Figure 9. In practice the partial derivatives required for the linear least-squares fit are estimated by stepping each parameter in turn and computing the shift in the field for each feature, $(\partial B/\partial P_i)_j \cong (\delta B/\delta P_i)_j$.

This approach usually works quite well, converging in several iterations. When difficulties occur, it is most likely due to the misassignment of experimental features to nuclear spin quantum numbers. An assignment which appears to make sense for an initial trial set of parameters may become nonsensical when the parameters are changed. Thus the program must be highly interactive with the user maintaining considerable control. In particular the opportunity to change assignments must be offered on each iteration of the program.

Very few experimental spectra exhibit all the features which might be predicted for an unbroadened powder pattern. There may also be features which, at least at an early stage of refinement, cannot be unambiguously assigned to a set of quantum numbers. For these reasons, the program does not require assignment of an experimental feature for every predicted feature.

Constraints can sometimes be applied to parameters in a spectrum analysis. For example, if the isotropic g-value is known, it might be appropriate to constrain g_x, g_y, and g_z by

$$\langle g \rangle = (g_x + g_y + g_z)/3$$

In some cases, it is appropriate to assume axial symmetry for one or more of the parameter matrices or to assume that two nuclei are magnetically equivalent. These various constraints can be built into the fitting program rather easily by stepping more than one parameter (in appropriate ways) in computing the partial derivatives for use in the least-squares routine. Early in an analysis, it is often true that one or more of the parameters influences the assigned features only to second order. In such a case, the least-squares fit will almost certainly "blow up" if these parameters are allowed to vary. Thus the program must allow for fixed parameters.

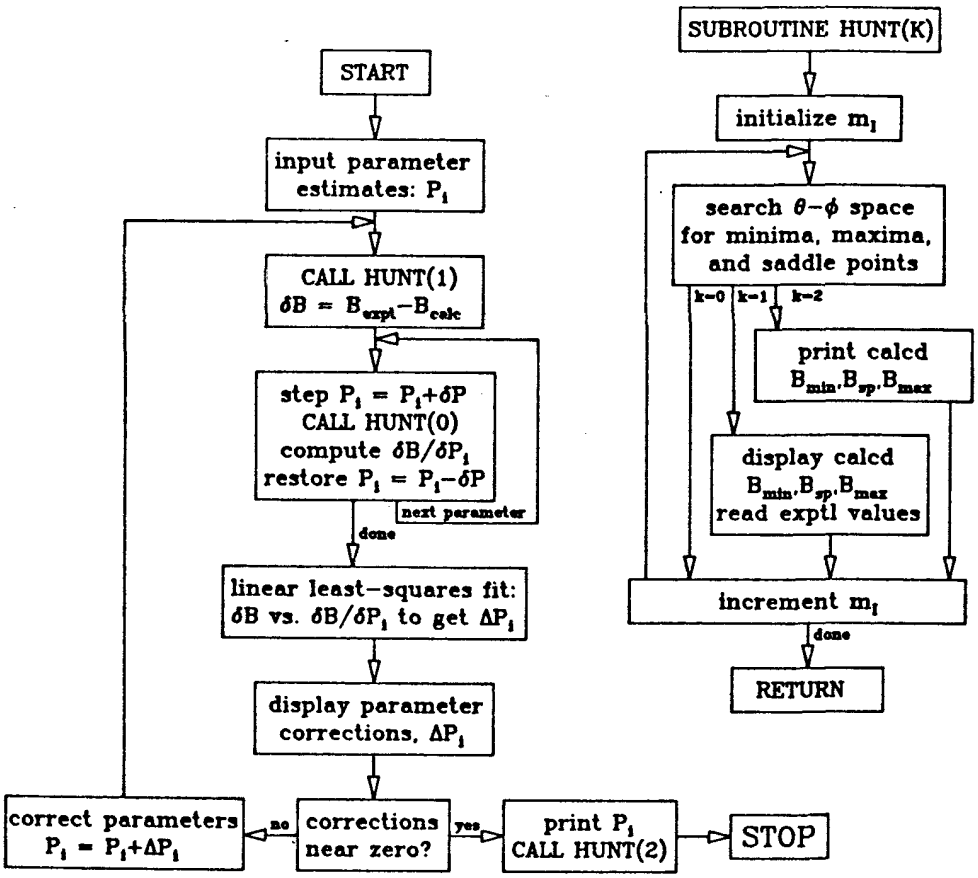

Figure 9. Block diagram of least-squares powder pattern fitting program.

Table 1. Non-Linear Least-Squares Fit of Line Positions

Iter.	g_x	g_y	g_z	$A_x/10^{-4}$ cm^{-1}	$A_y/10^{-4}$ cm^{-1}	$A_z/10^{-4}$ cm^{-1}	σ/G
0	2.040	2.060	2.250	30.0	10.0	195.0	16.6
1	2.051	2.054	2.252	38.0	15.5	192.6	10.6
2	2.053	2.054	2.252	27.2	20.0	193.4	2.8
3	2.053	2.057	2.251	27.0	19.8	193.5	0.9
4	2.053	2.057	2.251	26.8	19.9	193.5	0.8
5	2.053	2.057	2.251	26.7	20.1	193.5	0.7

Fit after five iterations:

m_I	Minima	Saddle Points	Maxima
3/2	2738 (2738.6)	3260 (3260.0)	3263 (3264.7)
1/2	2923 (2922.5)	3279 (3278.4)	3282 (3281.7)
-1/2	3107 (3106.7)	3309 (3307.8)	3315 (3315.2)
-3/2	3291 (3290.9)	3344 (3343.7)	3378 (3378.9)
	3326 (3326.5)	3371 (3371.6)	

As a simple illustration of the least-squares method, the powder pattern spectrum of copper(II) acetylacetonate was simulated using the parameters of Ovchinnikov and Konstantinov (6):

$$g_x = 2.0527 \quad g_y = 2.0570 \quad g_z = 2.2516$$
$$A_x = 27.0 \quad A_y = 19.5 \quad A_z = 193.4$$
$$(\times 10^{-4}\ cm^{-1})$$

The simulated spectrum shows fourteen assignable features, including two "extra lines" corresponding to $m_I = -3/2$. The spectrum, together with the positions of the features (to ± 1

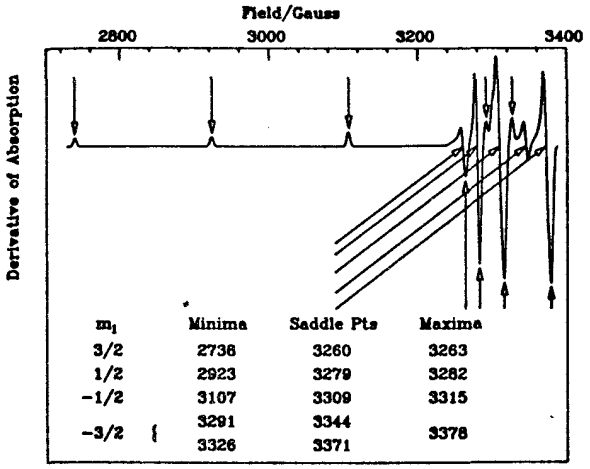

m_I	Minima	Saddle Pts	Maxima
3/2	2736	3260	3263
1/2	2923	3279	3282
-1/2	3107	3309	3315
-3/2	3291	3344	3378
	3326	3371	

Figure 10. Simulated spectrum of $Cu(acac)_2$ and measured field positions of resolved features.

G), is shown in Figure 10. These field positions were used in the non-linear least-squares program with an arbitrarily chosen set of initial parameters with the results shown in Table 1. Convergence was obtained in five iterations with an overall fitting error, σ = 0.7 G. The spin Hamiltonian parameters obtained from the least-squares fit were in satisfactory agreement with those used in the original simulation.

Work is currently in progress to extend this least-squares approach to the analysis of spectra influenced by nuclear quadrupole coupling and to cases with S > 1/2.

REFERENCES

(1) B. M. Peake, P. H. Rieger, B. H. Robinson, and J. Simpson, *J. Am. Chem. Soc.* **1980,** *102,* 156.

(2) L. V. Casagrande, T. Chen, P. H. Rieger, B. H. Robinson, J. Simpson, and S. J. Visco, *Inorg. Chem.* **1984,** *23,* 2019.

(3) J. A. DeGray, Meng Qin-Jing, and P. H. Rieger, to be published.

(4) D. L. Griscom, P. C. Taylor, D. A. Ware, and P. J. Bray, *J. Chem. Phys.* **1968,** *48,* 5158.

(5) P. H. Rieger, *J. Mag. Reson.* **1982,** *50,* 485.

(6) I. V. Ovchinnikov and V. N. Konstantinov, *J. Mag. Reson* **1978,** *32,* 179.

(7) W. E. Geiger, P. H. Rieger, B. Tulyathan, and M. D. Rausch, *J. Am. Chem. Soc.* **1984,** *106,* 7000.

(8) W. C. Hamilton, "Statistics in Physical Science," New York: Ronald Press, 1964.